X CONGRESSO NACIONAL DE ENGENHARIA MECÂNICA 2018
20 A 24 DE MAIO DE 2018 SALVADOR – BA – BRASIL

A numerical study on fatigue life predictions based on nominal and local approaches

Luiz Carlos de Andrade Ribeiro Junior, luiz.ribeirojunior@globomail.com[1]
Jorge Alberto Rodriguez Duran, jorge.a.r.duran@gmail.com[1]

[1]Volta Redonda School of Metallurgical Engineering, Federal Fluminense University, Volta Redonda 27255-125, Rio de Janeiro, Brazil

Abstract: *The aim of the present paper is to highlight the advantages of the local strain-based approach ϵN for fatigue assessment of notched components over the more traditional stress-based approach σN. A brief theoretical explanation is followed by a comparison between the predicted fatigue life for these two approaches for a group of 60 ductile structural steels under uni-axial constant stress amplitude. Hypothetical notched parts with different stress concentration factors SCFs in the range of 1.5 to 4.0 were used. The minimum to maximum load ratio R was kept constant and equal to 0.1. In order to focus the comparison on the local stress-strain analysis, the simulation was limited to the nominal elastic regime where both methods use the same fatigue strength curve. With this aim, the σ_{an} to σ_o ratio remained between 0.1 and 0.4. Also, the same function to account for the mean stress effects was incorporated in both approaches in such a way that fatigue strength curves for different mean loads were collapsed, for a given stress ratio (normally $R = -1$), towards the σ_{an} direction. The results are expressed in universal graphs with the σ_{an}/σ_o ratio in the abscissa and the $N_f - ratio$ in the ordinates. The $N_f - ratio$ is defined as the quotient between the N_f predictions according to the σN and ϵN approaches, considering the average values for the group of 60 structural steels in each load level. For low SCFs the $N_f - ratio$ has a trend to fall below the unity as the load level increases. This trend also remains for high SCFs until a σ_{an}/σ_o ratio around 0.3 but reverses for high load levels. Both scenarios result from the improved local stress-strain analysis performed under the strain-based approach and confirm its advantages for fatigue life assessment.*
keywords: *fatigue strain-based approach, strain-life curves, elastic-plastic stress-strain analysis*

1. INTRODUCTION

Fatigue life assessment models can be broadly divided in two groups: those based on stress/strain strength curves (or fatigue crack propagation strength curves) and those based on a fatigue damage parameter which is calculated on each cycle (Santecchia *et al.*, 2016). The present paper focused on the first group of models. Since the intrinsic characteristics of the fatigue cracks nucleation process are different from the fatigue crack growth process, different approaches have been developed in each stage (Kopas *et al.*, 2017). In the engineering community, the most popular models in the nucleation phase are those based on nominal stresses (the σN approach) or local strains analysis (the ϵN approach). In the crack propagation phase the favorite model is based on linear elastic fracture mechanics *LEFM* (the $da/dN\ vs.\ \Delta K$ approach) (Duran and Hernandez, 2014). These methods were occasionally combined in the past. For example, models for fatigue crack growth were developed and tested from the strain-based approach (Duran *et al.*, 2003). A unified model, which is a combination of the strain-based and fracture mechanics-based approaches (Noroozi *et al.*, 2005) was also proposed that time. This unified model has been recently applied to welded structures (Mikheevskiya *et al.*, 2015). Obviously, there are many examples of fatigue life assessment using the stress, strain and *LEFM* models individually. For example, in the case of notched specimens submitted to laboratory tests using a standardized helicopter load spectrum, all the aforementioned approaches have predicted fatigue lives with reasonable accuracy (Everett, 1990).

The objective of the present research is to graphically compare the fatigue life predictions according to the stress and strain based approaches. In this way, it is intended to highlight the advantages of the strain-based approach over the more traditional stress-based approach for fatigue life assessment.

2. FATIGUE STRENGTH CURVES

The stress-based approach is essentially an empirical method based on the relation between the stress amplitude σ_a and the number of cycles $N_f^{\sigma N}$ for complete failure of small specimens. Two fitting constants or materials properties (σ'_f and b) are needed to relate these parameters and the resulting equation is considered the fatigue strength under zero mean stress for a given material.

$$\sigma_a = \sigma'_f \left(2N_f^{\sigma N}\right)^b \tag{1}$$

Note that σ'_f is the failure stress in one reversal or the curve intercept in $N_f^{\sigma N} = \frac{1}{2}$ cycles, while b is the slope of the same curve. Typical values for an SAE 1015 steel are $\sigma'_f = 1020\,MPa$ and $b = -0.138$ (Dowling *et al.*, 2009). Some materials exhibit a rise in slope b of the curve described by equation 1, mainly above 10^7 cycles, reaching to $b = 0$ in some cases, which has been interpreted as a fatigue limit σ_e. More recent studies suggest that in the so-called giga-cycle fatigue regime ($Nf >\approx 10^8 cycles$) the fatigue strength continues to decrease (Sadananda *et al.*, 2007), in spite of the fact that the nucleation mechanism changes. Under very particular circumstances of dynamic loading, the fatigue design for a particular life N_f simply consists in comparing the nominal stresses acting on the component and scaled by a safety factor X_S with the fatigue resistance expressed in the form of equation 1. Those circumstances could be, for example, uni-axial completely reversed stresses of constant amplitude and no stress concentration. Machine parts and structures however, are seldom exposed to the above conditions and new functions accounting for stress concentration at notches, multi-axial stresses, mean stresses, variable amplitude loading and damage accumulation must be used. All of these issues were dealt with in detail in a previous paper (Duran and da Costa, 2016) but will be reviewed in this paper as well (see below).

On the other hand, local approaches have found wide acceptance to model the fatigue phenomenon mainly because the damage process that leads to this type of failure is highly localized. The philosophy underlying the fatigue strain-based approach is simple: the local cyclic strain history in regions of stress concentration, being experimentally related to the number of fatigue cycles, can be used as a parameter for design purposes (Stephens *et al.*, 2000). The robustness of the strain as a fatigue parameter is enhanced in the elastic-plastic regime and for materials with low strain hardening characteristics. Nevertheless the local strain-based approach for fatigue analysis is also adequate in the high cycle fatigue regime. Even when most part of the component is under elastic conditions, some volumes, mainly in the neighborhood of the unavoidable notches, can undergo plastic deformation. No matter the model that is used for defining fatigue damage, i.e. the degradation in ductility properties of the material due to cyclic slip of crystal grains (Murakami, 2012) or the behavior of small cracks (Murakami *et al.*, 2016) (Murakami and Miller, 2005), the Coffin-Manson equation still convincingly represents the strain versus number of cycles for most of the experimental data of metallic materials. This is simply an extension to the elastic-plastic regime of equation 1. For uni-axial loading in the first principal direction this relation is:

$$\epsilon_a = \frac{\sigma'_f}{E}\left(2N_f^{\epsilon N}\right)^b + \epsilon'_f\left(2N_f^{\epsilon N}\right)^c \tag{2}$$

In equations 1 and 2 σ'_f and ϵ'_f are the fatigue strength and ductility coefficients, respectively, while b and c are the corresponding fatigue exponents. Laboratory uni-axial strain-controlled tests, normally performed under a constant minimum to maximum strain ratio $R = \epsilon_{min}/\epsilon_{max} = -1$, provides the necessary set of ϵ_a and N_f data to determine the fatigue coefficients and exponents in equation 2.

3. STRESS ANALYSIS

Stress analysis under the σN approach is totally developed in the elastic regime. The nominal stress amplitude S_a is either calculated by elementary analytic formulas or by numerical techniques. For notched bodies, the local stress amplitude is calculated simply scaling the nominal stress by the elastic stress concentration factor K_t. Solutions for K_t are available in the form of equations or charts that have been derived from the elasticity theory. They are always presented in a non-dimensional form being, therefore, size-independent. Stress concentration factors depend, however, on the geometry and mode of loading. For ductile materials, a conservative procedure consists in dividing the fatigue strength of equation 1 by the *SCF*:

$$S_a = \frac{\sigma_a}{K_t} = \frac{\sigma'_f\left(2N_f^{\sigma N}\right)^b}{K_t} \tag{3}$$

Under linear elastic conditions the perturbation originated by the *SCF* tends to vanish quickly by equilibrium requirements. For this reason a high stress gradient exist and only a small volume of material is under the influence of peak stresses. As a result, the fatigue strength of notched specimens is above the expected S_a value based on equation 3. This is more evident in the near-threshold fatigue region and a fatigue notch reduction factor K_f has been introduced. Both classical (Pilkey and Pilkey, 2008) and modern (Atzori *et al.*, 2003) formulations for K_f exist, the latter being recommended for crack-like (or very sharp) notches. Nevertheless, the use of the *SCF* in its traditional form is always conservative and so it will be done here.

Mean loads has a detrimental effect on fatigue strength but they are normally included in the stress analysis. In 1970 Smith et. al. (Smith *et al.*, 1970) proposed that the fatigue life nucleation $g(N_f)$ is controlled by the product between the maximum stress σ_{max} and the strain amplitude ϵ_a, independently of the mean load.

$$g(N_f) = \sigma_{max} \cdot \epsilon_a \tag{4}$$

The quantity $\sigma_{max} \cdot \epsilon_a$ is proportional to the strain energy density thus the so-called *SWT* modification can be viewed as an energetic approach. It is possible to relate equation 4 with equation 1 through the following reasoning: if the $g(N_f)$

function is valid for any mean load, it will be valid for $R = -1\,(\sigma_m = 0)$ and therefore equal to the product σ_a^2/E as follows:

$$g(N_f) = \sigma_{max} \cdot \epsilon_a = (\sigma_m + \sigma_a)\frac{\sigma_a}{E} = \frac{\sigma_a^2}{E} \tag{5}$$

Note that in equation 5 a uni-axial stress state has been considered since the substitution $\epsilon_a = \sigma_a/E$. Under these circumstances, i.e. completely reverse loading ($R = -1$) and uni-axial stress state, the stress amplitude in equation 5 is the same as in equation 1. Defining the *SWT* parameter as $P_{SWT} = \sigma_{max} \cdot \epsilon_a$ we have:

$$P_{SWT}^{\sigma N} = \frac{(\sigma_f')^2}{E}\left(2N_f^{\sigma N}\right)^{2b} \tag{6}$$

The P_{SWT} is widely used to include the mean stress effects on fatigue life calculations. It is expected that data for various mean loads be condensed in a unique curve in $P_{SWT}\, vs.\, 2N_f$ coordinates. It is also possible to think on the *SWT* as a method that computes a equivalent completely reversed stress amplitude σ_{ar} from any combination of σ_a and σ_m as follows (see equation 5):

$$\sigma_{ar} = \sqrt{\sigma_a^2 + \sigma_a \cdot \sigma_m} \tag{7}$$

All that remains is to equate equations 7 and 1 for design purposes. Moreover, since no distinction was made between notched and un-notched bodies to obtain the P_{SWT} parameter, equation 7 can also be expressed in terms of nominal stresses.

$$S_{ar} = \sqrt{S_a^2 + S_a \cdot S_m} \tag{8}$$

The combined effects of mean stresses and *SCFs* can now be dealt with after substituting this result in equation 3:

$$S_{ar} = \frac{\sigma_{ar}}{K_t} = \frac{\sigma_f'\left(2N_f^{\sigma N}\right)^b}{K_t} = \sqrt{S_a^2 + S_a \cdot S_m} \tag{9}$$

For brittle materials it will be necessary to multiply the nominal mean stress component S_m in equation 9 by a *SCF* for mean loads K_{tm} which vary according to the nominal maximum stress S_{max} (Dowling, 2013). All the steels used in the present research are classified as ductile materials and so it was not necessary to introduce the K_{tm}. The predicted life by the stress-based approach $N_f^{\sigma N}$ can now be calculated by equation 9 for a given combination of nominal stress amplitude and mean (or equivalently *R*) and *SCF*.

The strain-life curves (equation 2) are also sensitive to mean loads. The same mean load function, i.e. the *SWT* parameter should be used in order to meet the objectives of the present research. The logic to introduce the P_{SWT} is similar to that previously used for stress-life curves. First note that in equation 5 the $g(N_f)$ function for uni-axial stress state and zero mean stress can be expressed in terms of local stresses and strain amplitudes:

$$g(N_f) = \sigma_{max} \cdot \epsilon_a = \sigma_a \cdot \epsilon_a \tag{10}$$

Introducing both equations 1 and 2 into equation 10 results in the $P_{SWT}\, vs.\, N_f$ relation that, theoretically should fit the strain-life data for any mean load.

$$P_{SWT}^{\epsilon N} = \frac{(\sigma_f')^2}{E}\left(2N_f^{\epsilon N}\right)^{2b} + \epsilon_f'\,\sigma_f'\left(2N_f^{\epsilon N}\right)^{b+c} = \sigma_{max} \cdot \epsilon_a \tag{11}$$

Life calculations according to the strain-based approach to obtain $N_f^{\epsilon N}$ using the same combination of nominal stress amplitude, nominal mean stress and *SCF* used in the stress-based approach can now proceed, as long as the local values of σ_{max} and ϵ_a of equation 11 are known. It is exactly at this point that main differences between the two approaches emerge. In the $\epsilon\, N$ approach, a elastic-plastic analysis is performed to determine local stresses and strains. These local values can be directly related to the applied stresses (and consequently to the external loads) through the stabilized cyclic stress-strain curve of the material. For many materials, equations that have the Ramberg-Osgood form can be used to represent these curves:

$$\epsilon_a = \frac{\sigma_a}{E} + \left(\frac{\sigma_a}{H'}\right)^{\frac{1}{n'}} \tag{12}$$

where E is the Young's modulus, H' and n' are the cyclic strength coefficient and cyclic strain hardening exponent, respectively. These parameters are fitted to a set of uni-axial stress and strain amplitude values corresponding to stabilized hysteresis loops, usually at the half-life stage of the strain-life tests. Some alternative methods consist in using only one specimen submitted to multiple steps of increasing or decreasing amplitude strains (Jones and Hudd, 1999). In the case of notched members in plane stress, in addition to the cyclic stress-strain curve , the amplitude strains should also satisfy

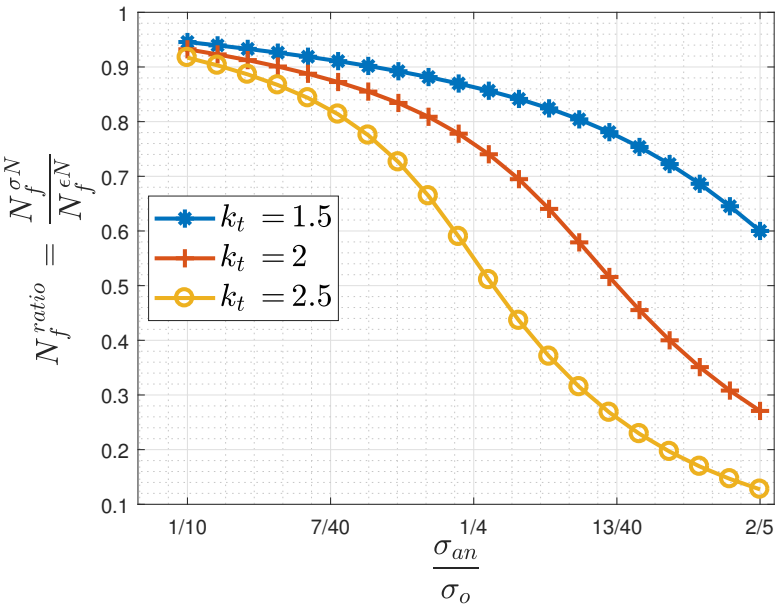

Figure 1: Variation on the ratio of life predictions (average values) from the σN approach to the ϵN approach for a group of 60 ductile structural steels at different nominal constant amplitude stress levels. Pulsating loads with $R = 0.1$ and low *SCFs* were used.

some approximated strain distributions such as those proposed by Neuber (Neuber, 1961) and Glinka (Glinka, 1985). The former will be used in the present paper and its mathematical form is:

$$\epsilon_a \cdot \sigma_a = \frac{(K_t \cdot S_a)^2}{E} \tag{13}$$

The values of σ_a and ϵ_a (or σ_{max} and ϵ_{max}) that simultaneously satisfy the system of non-linear equations 12 and 13 are the local quantities needed to be entered in equation 11 for life-calculations. Numerically it is preferably to eliminate ϵ_a from equations 12 and 13, calculate by iteration the σ_a for a given S_a and K_t and then use the result in either, equation 12 or equation 13 to obtain ϵ_a. The same procedure should be used to calculate the maximum local values, the only difference being the use of the maximum nominal value S_{max} instead of the S_a in the system of equations.

4. METHODOLOGY

Both fatigue life prediction approaches aforementioned have been implemented as MatLab functions. Then, a hypothetical design (or assessment) situation consisting of a loaded notched member with different stress concentration factors *SCFs* (between 1.5 and 4) has been considered. The monotonic and cyclic properties of 60 ductile structural steels have been gathered (Boller and Seeger, 1987) and used as input parameters for these functions. For each material, the member is considered as loaded, one at a time, by a vector of constant nominal stress amplitudes σ_{an} normalized in relation to the material's yield strength σ_o. The σ_{an}/σ_o ratio spans between 0.1 and 0.4. A constant load ratio $R = \sigma_{min}/\sigma_{max} = 0.1$ was used. For each material, level of normalized load and group of *SCF*, the average value of the ratio between the σN and ϵN life predictions, defined as the N_f^{ratio}, was calculated and recorded for plotting. Other important quantities such as the ratio between local amplitudes and mean strains and stresses by each method, which allows a better understanding of the trends in the N_f^{ratio}, were also calculated and plotted.

5. RESULTS AND DISCUSSION

Figures 1 and 2 show the graphs of the average N_f^{ratio} versus the normalized load applied for a group of 60 steels. As noted before, the behavior of the N_f^{ratio} differs for low and high *SCFs*. In the first case the σN life predictions $N_f^{\sigma N}$ are persistently lower than the ϵN predictions $N_f^{\epsilon N}$. Both the increase in the normalized load level and the *SCF* reinforce this behavior. The same trend is maintained for the second case but there is an inflection point when the combination of high loads and notch severity causes a decrease in the strain-based life predictions.

In a broad sense, both behaviors are explained by the inherent difficulties of a purely linear elastic stress analysis, such as that carried out in the σN approach, to deal with local stresses and strains that are probably in the frontier (or within) of the elastic-plastic regime. Through the use of a combination of equations (12 and 13) the ϵN approach enables the use of more realistic stresses and strains for life predictions.

A further insight about the differences in life predictions can be gained if the ratio between local amplitude and mean strains by each method (average values for all materials studied), are now plotted for each load level (see figure 3). For this plot the *SCF* was fixed in $K_t = 2$ while the load ratio was the same as before i.e. $R = 0.1$. As can be seen in the figure, the local strain amplitude ratios are approximately the same for almost the entire vector of loading, but the local

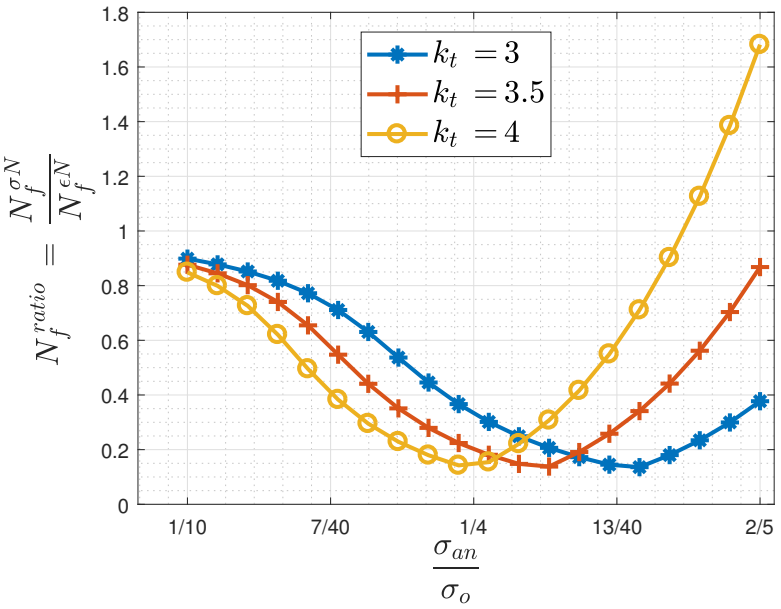

Figure 2: The same results presented in figure 1 now using high values of the *SCF*.

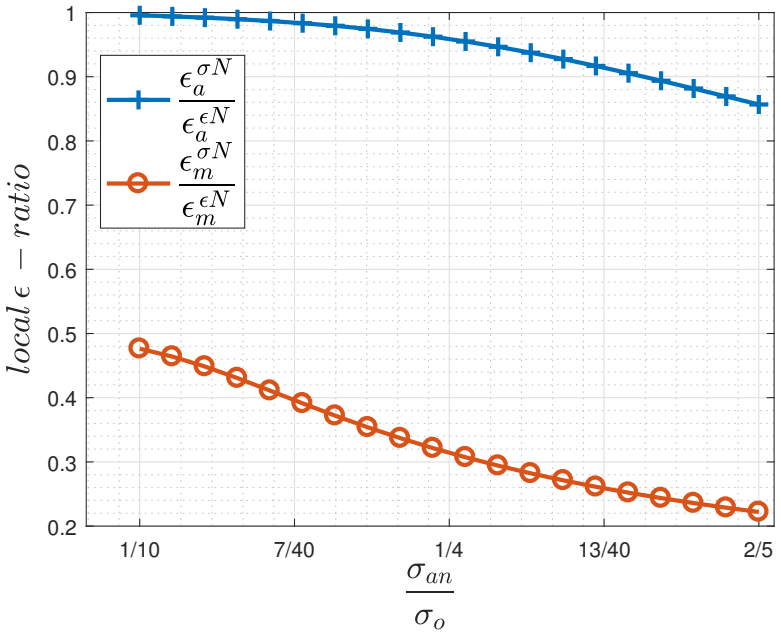

Figure 3: The average values for all materials studied for the ratio between local amplitude and mean strains by each approach for a fixed $K_t = 2.0$

mean strains by the ϵN method, $\epsilon_m^{\epsilon N}$ are always well above than the local mean strains by the σN method. The average local mean stresses $\sigma_m^{\epsilon N}$, on the other hand, follow a opposite trend (see figure 4), as expected by the non-linear relation between these variables expressed by equation 12.

The stress strain analysis performed under the ϵN approach deserves a deeper exploration. If the combination of nominal load and K_t in a cycle is high enough to induce local stresses and strains in the plastic regime, and both quantities are estimated and plotted against in a common locus, the result is a hysteresis loop. As an example, figure 5 shows this estimated stress-strain paths (hysteresis loops) at four normalized load levels for the AISI 1141 steel (199 HB) and $K_t = 2$. While the σ_{an}/σ_o ratio grows by around 122 % (0.4/0.18=2.22) the estimated local mean stress grows only 13 %. The analysis of figures 4 and 5 leave no doubts about the more rational treatment of the mean load effects on fatigue carried out in the context of the ϵN approach.

The strain energy density associated with thicker loops is obviously higher than that calculated for thinner loops. A plot of the average ratio $P_{SWT}^{\epsilon N}/P_{SWT}^{\sigma N}$ versus the normalized load, still for AISI 1141 steel (figure 6) shows, however a growing trend. Despite of the fact that the $P_S^{\epsilon N}WT$ parameter becomes more realistic in the context of the ϵN approach, mainly as the normalized load grows, the poor stress analysis in the context of the σN approach generates a $P_S^{\sigma N}WT$ parameter that is absurdly high and unrealistic, thus explaining the shown trend. Although the $P_{SWT}vs.N_f$ curves are different by each approach (see figure 7), a lower or more realistic driving force (or $P_{SWT}^{\epsilon N}$ parameter) results in a longer predicted life, what constitutes an additional explanation for the average results shown in figure 1.

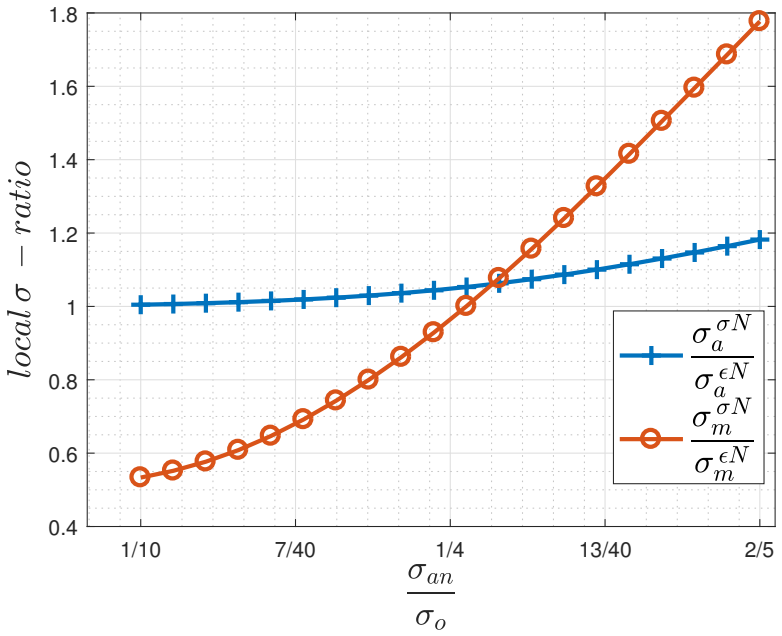

Figure 4: The average values for all materials studied for the ratio between local amplitude and mean stresses by each approach for a fixed $K_t = 2.0$

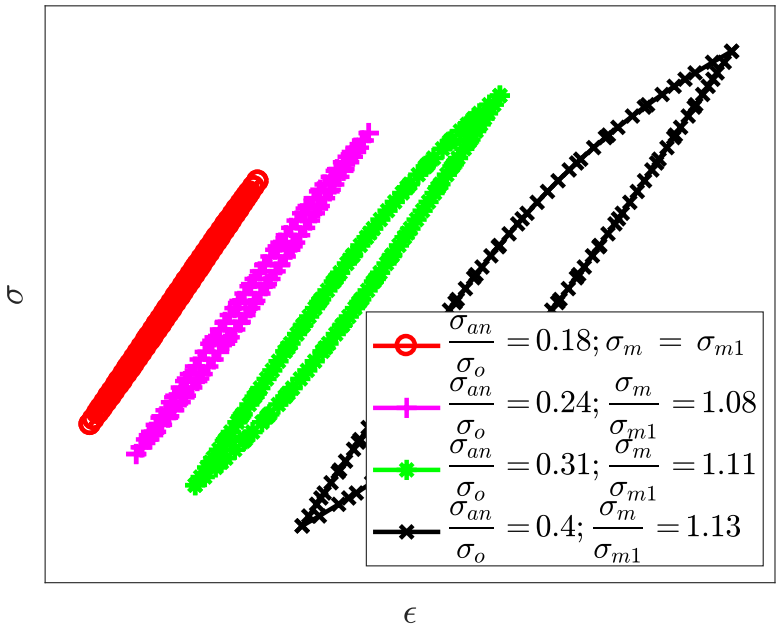

Figure 5: Estimated stress-strain path (hysteresis loops) by the ϵN approach at four normalized load levels for the AISI 1141 steel (199 HB) and $K_t = 2$.

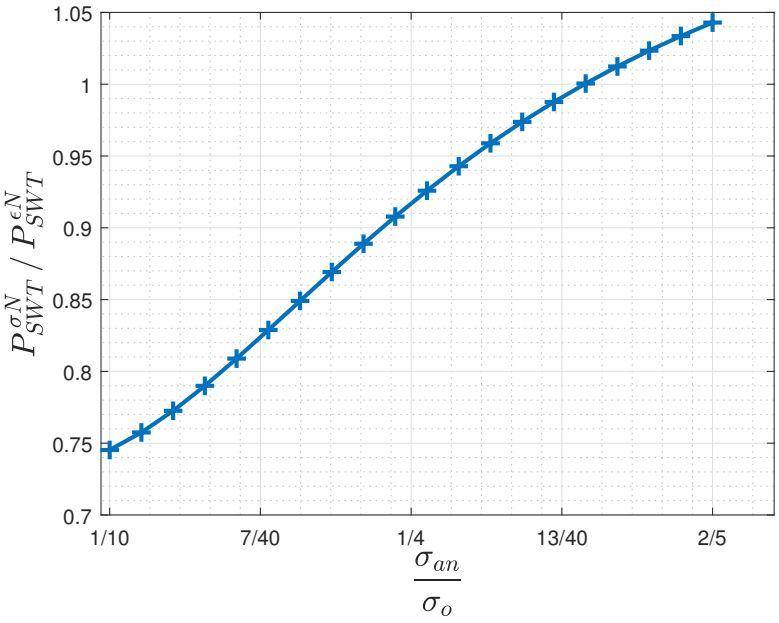

Figure 6: The ratio between the P_SWT parameters, $P_{SWT}^{\epsilon N}/P_{SWT}^{\sigma N}$ grows along with the normalized load for the AISI 1141 steel (199 HB) and $K_t = 2$.

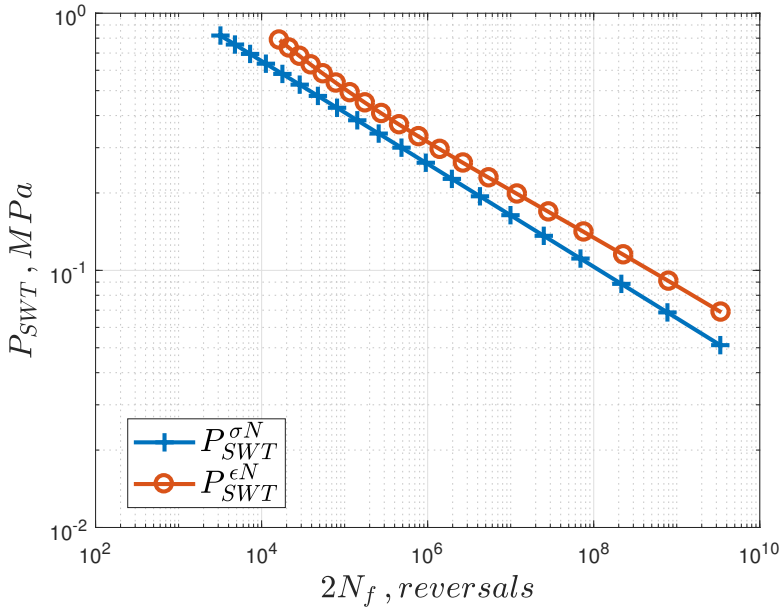

Figure 7: The $P_{SWT} vs. N_f$ curves for the AISI 1141 steel (199 HB) and $K_t = 2$ by the two approaches.

6. CONCLUSIONS

The numerical simulation performed in the present paper has demonstrated that, by virtue of a more realistic and accurate stress analysis, by employing local values instead of nominal ones, the strain-based approach performs, in average, less conservative life predictions than the more traditional stress-based approach for a group of 60 ductile structural steels.

7. References

Atzori, B., Lazzarin, P. and Meneghetti, G., 2003. "Fracture mechanics and notch sensitivity". *Fatigue & Fracture of Engineering Materials & Structures*, Vol. 26, No. 3, pp. 257–267. ISSN 1460-2695. doi:10.1046/j.1460-2695.2003.00633.x. URL `http://dx.doi.org/10.1046/j.1460-2695.2003.00633.x`.

Boller, C. and Seeger, T., 1987. *Materials data for cyclic loading*. Materials Science Monographs 42A, Elsevier Science, The Netherlands.

Dowling, N.E., 2013. *Mechanical Behavior of Materials: Engineering Methods for Deformation, Fracture and Fatigue*. Pearson Education Limited, fourth edition edition.

Dowling, N.E., Calhoun, C.A. and Arcari, A., 2009. "Mean stress effects in stress-life fatigue and the walker equation". *Fatigue Fract. Engng. Mater. Struct.*, Vol. 32, pp. 163–179. doi:10.1111/j.1460-2695.2008.01322.x.

Duran, J. and da Costa, D., 2016. "An evaluation of the nominal stress method for life prediction of cylindrical circumferential v-notched specimens tested under variable amplitude loading". *Applied Mechanics and Materials*, Vol. 851, pp. 310–316. doi:10.4028/www.scientific.net/AMM.851.310.

Duran, J.A.R., Castro, J.T. and da Cruz Payão Filho, J., 2003. "Fatigue crack propagation prediction by cyclic plasticity damage accumulation models". *Fatigue & Fracture of Engineering Materials & Structures*, Vol. 26, pp. 137–150. doi:10.1046/j.1460-2695.2003.00630.x.

Duran, J.A.R. and Hernandez, C.T., 2014. "Evaluation of three of the current methods for including the mean stress effect in fatigue crack growth rate prediction". *Fatigue & Fracture of Engineering Materials & Structures*, Vol. 38, No. 4, pp. 410–419. doi:10.1111/ffe.12242.

Everett, R., 1990. "A comparison of fatigue life prediction methodologies for rotorcraft". Technical report, Nasa Technical Memorandum 102759.

Glinka, G., 1985. "Energy density approach to calculation of inelastic strain-stress near notches and cracks". *Engineering Fracture Mechanics*, Vol. 22, No. 3, pp. 485 – 508. ISSN 0013-7944. doi:https://doi.org/10.1016/0013-7944(85)90148-1. URL `http://www.sciencedirect.com/science/article/pii/0013794485901481`.

Jones, A. and Hudd, R., 1999. "Cyclic stress-strain curves generated from random cyclic strain amplitude tests". *International Journal of Fatigue*, Vol. 21, No. 6, pp. 521 – 530. ISSN 0142-1123. doi:https://doi.org/10.1016/S0142-1123(99)00014-6. URL `http://www.sciencedirect.com/science/article/pii/S0142112399000146`.

Kopas, P., Saga, M., Baniari, V. and et.al, 2017. "A plastic strain and stress analysis of bending and torsion fatigue specimens in the low-cycle fatigue region using the fem". *Procedia Engineering*, Vol. 177, pp. 526–531.

Mikheevskiya, S., Glinka, G. and Cordes, T., 2015. "Total life approach for fatigue life estimation of welded structures". *Procedia Engineering*, Vol. 101, pp. 177–184. doi:10.1016/j.proeng.2015.02.023.

Murakami, S., 2012. *Continuum Damage Mechanics: a continuum mechanics approach to the analysis of damage and fracture*. Springer.

Murakami, Y., Ferdous, M. and Makabe, C., 2016. "Low cycle fatigue damage and critical crack length affecting loss of fracture ductility". *International Journal of Fatigue*, Vol. 82, pp. 89–97.

Murakami, Y. and Miller, K., 2005. "What is fatigue damage? a view point from the observation of low cycle fatigue process". *International Journal of Fatigue*, Vol. 27, pp. 991–1005.

Neuber, H., 1961. "Theory of stress concentration for shear-strained prismatic bodies with nonlinear stress-strain law". *Journal of Applied Mechanics*, Vol. 28, No. 4, pp. 544–550.

Noroozi, A., Glinka, G. and Lambert, S., 2005. "A two parameter driving force for fatigue crack growth analysis". *International Journal of Fatigue*, Vol. 27, pp. 1277–1296. doi:10.1016/j.ijfatigue.2005.07.002.

Pilkey, W. and Pilkey, D., 2008. *Peterson's stress concentration factors*. John Wiley & Sons Inc, third edition edition.

Sadananda, K., Vasudevan, A. and Phan, N., 2007. "Analysis of endurance limits under very high cycle fatigue using a unified damage approach". *International Journal of Fatigue*, Vol. 29, pp. 2060–2071.

Santecchia, E., Hamouda, A.M.S. and et. al., F.M., 2016. "A review on fatigue life prediction methods for metals". *Advances in Materials Science and Engineering*, Vol. 2016, pp. 1–27. doi:10.1155/2016/9573524.

Smith, K.N., Watson, P. and Topper, T.H., 1970. "A stress-strain function for the fatigue of metals". *Journal of Materials*, Vol. 5, No. 4, pp. 767–778.

Stephens, R., Fatemi, A., Stephens, R. and Fuchs, H., 2000. *Metal fatigue in engineering*. Wiley Interscience.

8. AUTHORS RESPONSIBILITY

The authors are the only one responsible for the content of this work.